Available online at www.sciencedirect.com
ScienceDirect
Journal of the European Ceramic Society 32 (2012) 149–156
www.elsevier.com/locate/jeurceramsoc

# Joining of SiC by Al infiltrated TiC tape: Effect of joining parameters on the microstructure and mechanical properties

Wu-Bian Tian *, Hideki Kita, Hideki Hyuga, Naoki Kondo

*National Institute of Advanced Industrial Science and Technology (AIST), 2266-98 Anagahora, Shimo-Shidami, Moriyama-ku, Nagoya 463-8560, Japan*

Received 15 February 2011; received in revised form 22 July 2011; accepted 1 August 2011
Available online 27 August 2011

**Abstract**

SiC ceramics were successfully joined by Al infiltrated TiC tapes at 900–1100 °C for 0.5–2 h in vacuum. Phase constituents, microstructure and mechanical strength of the prepared SiC joints were characterized. The prepared SiC joints display dense interlayer and crack-free interface. The interlayer primarily consists of TiC and Al phases, together with small amount of $TiAl_3$ and trace of $Al_4C_3$. With increasing the joining temperature or time, the interface layer either thickens or grows to multiple layers. The bending strengths of the SiC joints are higher than 190 MPa as bonded at present conditions, and are closely related with the property of interface and interlayer.


*Keywords:* Joining; Silicon carbide; Infiltration; Microstructure; Mechanical properties

## 1. Introduction

Silicon carbide (SiC) is one of the most widely used ceramic materials for structural applications because of its combination of exceptional properties, such as light weight, good mechanical properties (high hardness, strength and elastic modulus), low thermal expansion and high thermal conductivity.[1,2] For instance, the high specific strength and specific modulus of SiC make it a desirable candidate for stepper guide and wafer stage for semiconductor production.

SiC parts with small size and simple shape are commercially available. For producing large-size SiC components, joining is generally considered to be one of the promising and effective approaches.[3,4] Till now, various joining techniques have been applied to produce SiC parts, including brazing,[5–7] reaction joining,[8,9] green-state joining with polymer precursors[10–12] and diffusion bonding.[13] All these methods exhibit their merits for the given applications. For example, brazing is a conventional and pressureless joining method for relatively low temperature use whereas reaction joining and diffusion bonding can produce joints for use at much higher temperatures. In addition, melt infiltration is a conventional method to produce metal matrix composites (MMCs) and reaction-bonded SiC (RBSC). As far as we know, the successful bonding of SiC has been achieved by RBSC technique.[14–16] The joining of SiC with MMCs formed by melt infiltration, however, has rarely been reported.

In the present study, we focus on the joining of SiC with Al infiltrated titanium carbide (TiC) tape because it exhibits the following advantages: (1) Al melt shows good wetting with SiC and TiC ceramics[17–19]; (2) TiC incorporated Al interlayer probably yields high strength and modulus; (3) infiltration technique is a pressureless and low-cost process, generally requiring no noble metals. Our motivation, therefore, is to evaluate the possibility to bind SiC ceramics using Al melt infiltration process. The influences of joining parameters, such as temperature and time, on the microstructure and mechanical properties of SiC joints were investigated. In addition, the mechanisms of joining are also discussed.

## 2. Experimental procedure

The preparation of TiC preform and tape was similar to that in our previous work.[20,21] Briefly, TiC powders (Grade TiC-01, Japan New Metals Co. Ltd., Japan) with the addition of 1 wt.% dispersant and 3 wt.% binder were ball milled for 24 h in ethanol. The mixtures were dried with a rotary evaporator, crushed and screened through a 150 mesh sieve. Green com-

* Corresponding author. Tel.: +81 52 736 7120; fax: +81 52 736 7405.
*E-mail address:* w.b.tian@aist.go.jp (W.-B. Tian).

0955-2219/$ – see front matter. 
doi:10.1016/j.jeurceramsoc.2011.08.001

pacts, ~Φ20 mm × 5 mm, were formed by uniaxial pressing at about 32 MPa. Then the compacts were debinded at 600 °C in $N_2$ to pyrolyze the binder. The resulting TiC particulate preforms exhibited a green density of 2.6 g/cm$^3$, about 54% to the theoretical density of TiC (4.9 g/cm$^3$). Finally, the porous TiC preforms were infiltrated with aluminium melt at 800–1000 °C for 1 h in vacuum at a heating rate of 20 °C/min. For the preparation of TiC tape, its powders were dispersed with fuloren G700 (Kyoeisha Chemical Co., Japan) in a solvent of toluene and butanol, where polyvinybutyral (PVB) and dioctyl adipate (DOA) were used as the binder and plasticizer, respectively. Tape casting was conducted in a doctor blade (DR-150, Sayama Co. Ltd., Japan) with a blade gap of 300 μm and at a speed of 100 mm/min. The thickness of dry tape was about 46 μm.

SiC sintered bodies with a density of 3.1 g/cm$^3$ and a room-temperature bending strength of 450 MPa were purchased (Covalent Materials Co., Japan) and used in the present study. SiC plates were cut into a dimensions of 15 × 13 × 6 mm$^3$ and used for joining tests. Prior to joining, SiC plate surface (15 × 6 mm$^2$) was ground by 400# diamond wheel and ultrasonically cleaned in ethanol. The average surface roughness (Ra) of SiC was measured to be 0.13 μm. The TiC tape was sandwiched between two SiC plates and the sets were clamped by a graphite jig. About 0.1 g Al was put above the tape to obtain dense interlayer. Joining procedures were carried out at 900–1100 °C for 0.5–2 h in vacuum.

Phase constituents were determined by X-ray diffractometry (XRD, RINT2000, Rigaku, Japan) on the infiltrated bulk sample. The joined SiC samples were sectioned perpendicular to the interlayer and polished down to 0.5 μm diamond suspension. Microstructure observations on the polished surface and the fracture surface were performed via scanning electron microscope (JSM-5600, JEOL, Japan) equipped with energy dispersive spectroscopy (EDS JED-2300, JEOL, Japan). To determine porosity of the samples, quantitative analyses of SEM photographs were carried out using a free software ImageJ.[22] 3-point bending strength was measured on 4 × 3 × 26 mm$^3$ beams with a span of 20 mm at a crosshead speed of 0.5 mm/min. The tensile surfaces of the specimens were polished to a 0.5 μm diamond finish and the edges of tested specimens were bevelled. At least 3 specimens were used for the strength measurements.

## 3. Results and discussion

### 3.1. Infiltration of TiC preform by Al melts

Due to the difficulty to determine the phase constituents of a thin joint interlayer, we conducted the infiltration of Al melt to TiC preform and then carried out the XRD analysis and SEM observations on the bulk composite. Infiltration of Al into the TiC preforms was successful at 1000 °C, whereas it was unsuccessful at 800 °C. The corresponding XRD pattern of the infiltrated composite is shown in Fig. 1(a). Clearly, the prepared sample is composed of predominant TiC and Al phases as well as little amount of reaction-formed compounds like $TiAl_3$ and $Al_4C_3$. In the literature, the Al-based metal matrix composites and the wetting of TiC ceramics by Al melt had been extensively investigated.[23–25] The reactions between Al and TiC were found to be complicatedly affected by the preparation methods and processing parameters, generally producing new compounds including $TiAl_3$ and $Al_4C_3$ at a temperature lower than 1000 °C,[23,24] consistent with the results herein.

The low-magnification backscattered SEM (BSEM) image of the prepared sample, as shown in Fig. 1(b), exhibits some extinguished features. For instance, the microstructure consists of mainly gray areas and many bright needle-like ones with width of 10–25 μm and length of 50 μm to several hundred micrometers. The needles show obviously large size, high aspect ratio and bright contrast. At higher magnification, as presented in Fig. 1(c), the contrast difference between gray area and bright needles in Fig. 1(b) is attributed to the filled phase in TiC preforms.

A typical BSEM image of the gray area in Fig. 1(b) is given in Fig. 1(d), which consists of bright TiC phase and gray Al phase, as well as a few dark pores. Some white particles near or within pores originate from the metal debris of polishing plate. Fig. 1(e) shows the microstructure of a representative needle-shaped area (surrounded by the black dot lines), which contains bright TiC phases and light gray phases and a few micropores. EDS analysis suggests that the light gray areas are rich in Ti and Al elements (not shown here), which are most likely attributed to the $TiAl_3$ phase, as discussed below. The measured porosity of Fig. 1(d) is around 1.1% and that of the needle area in Fig. 1(e) is about 0.9%, therefore the prepared composite is nearly fully dense. The $Al_4C_3$ phase is hard to be distinguished from other phases under present examinations due to its small fraction. In fact, the needle-like $TiAl_3$ phase has been frequently observed in Al-2024 infiltrated TiC composites and spray deposited TiC/Al composites.[26,27] The reasons for the large-sized $TiAl_3$ grains are not clear now, but likely attributed to the fast growth and coalescence of smaller grains.

### 3.2. Joining of SiC by Al infiltrated TiC tapes

A SEM microstructural observation of SiC joint bonded at 1000 °C for 1 h by Al infiltrated TiC tape (i.e. joint TCA1060) is presented in Fig. 2(a), in which dense interlayer (porosity < 0.2%) with a thickness of 45 μm and crack-free interface between interlayer and SiC base can be seen. With a further examination at backscattered model and higher magnification, as shown in Fig. 2(b), we find that the microstructure within the interlayer is close to that of the bulk composite prepared at the same temperature, although the volume fraction of each phases might be varied with the preparation methods of TiC material. However, the interfaces at both sides are different in layer thickness and number. At the left side, the interface contains one light gray layer close to interlayer with a thickness around 3 μm (marked by I) and another dark gray layer near to SiC substrate with a thickness less than 1 μm (marked by II). On the other hand, there is only one dark gray layer at the right interface (marked by III).

EDS pattern indicates that the layer I (the white cross in Fig. 2(b)) is rich in Al element and mainly consists of pure

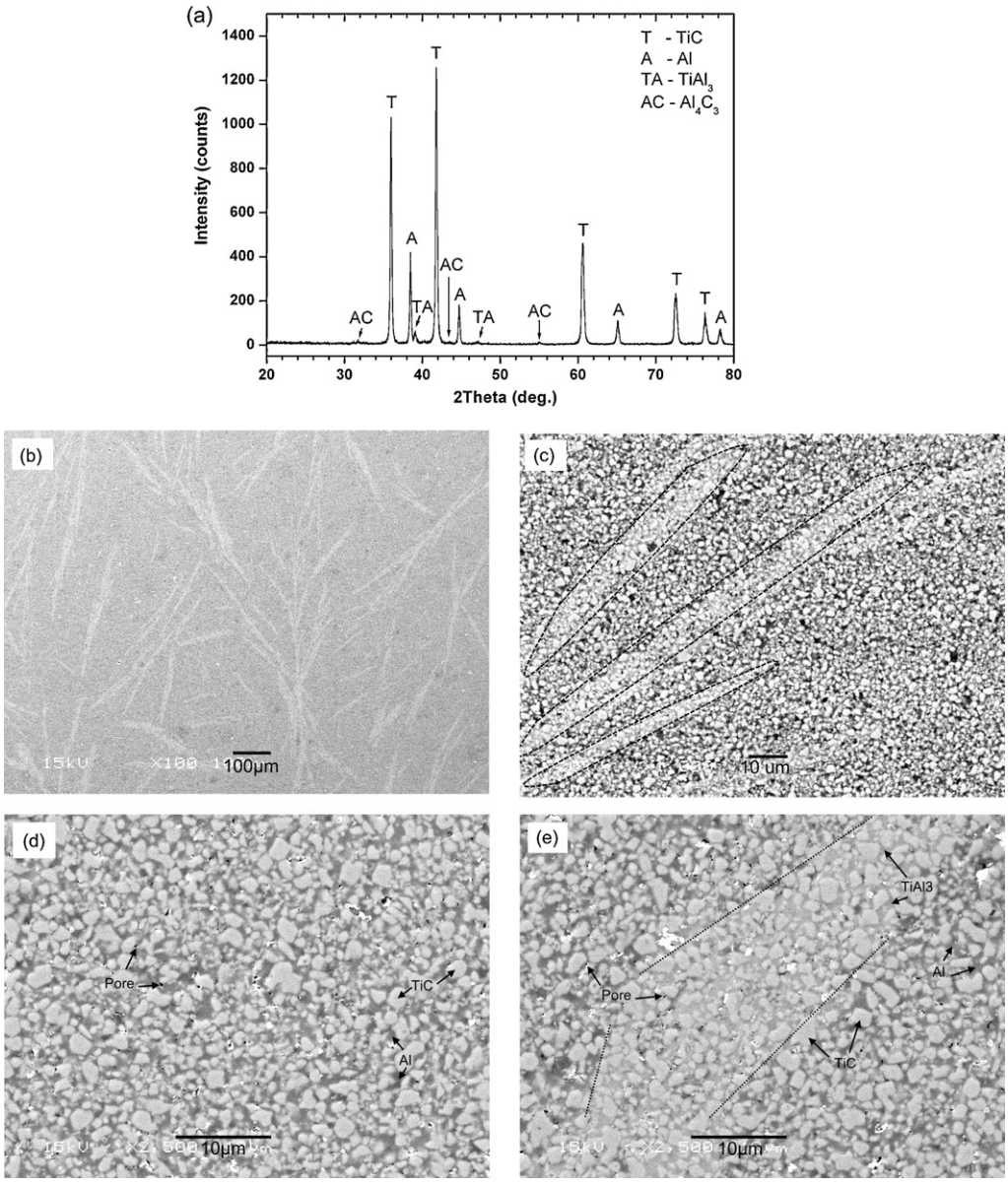


Fig. 1. (a) XRD pattern, (b) low-magnification and (c) higher magnification backscattered SEM examinations of TiC preform infiltrated by Al at 1000 °C for 1 h in vacuum. The typical BSEM images of: (d) the gray area and (b) the needle-shaped area in (b).

Al metal, as shown in Fig. 2(c). The formation of Al segregation layer is possibly related to the shrinkage of TiC tape and the fill of gap with melted Al during infiltration. The layers II and III are attributed to the reaction-formed productions between Al melt and SiC base, as discussed in Sections 3.3 and 3.4. In Fig. 2(b), we also find two needle-like areas within interlayer and mark them by black dot lines. One of them extends from interlayer to SiC substrate. At the downside of left interface, the needle-like grain (the black cross in Fig. 2(b)) does not contain TiC particles and its size is large enough for EDS analysis. The corresponding result, as presented in Fig. 2(d), suggests that the primary elements are Ti and Al, and the atomic ratio of Al to Ti is close to 3, verifying the presence of $TiAl_3$ phase. Note that the formed $TiAl_3$ phase shows good bonding behavior with both TiC and SiC.

### *3.3. Effect of joining parameters on the microstructure of SiC joints*

The observations of SiC joints bonded at different temperatures and dwelling time are presented in Fig. 3(a) through (d). We found that the microstructure within interlayer is independent of the joining temperature and time. The interfaces, however, vary significantly with joining conditions. As joined at 900 °C for 1 h (joint TCA960 in Fig. 3(a)) or 1000 °C for 0.5 h (joint TCA1030 in Fig. 3(c)), the interface microstructure of SiC joint is similar to that of TCA1060 (Fig. 2(b)), which is composed of a one-layer interface at one side and a two-layer structure at the other side. As the joining temperature increases to 1100 °C (joint TCA1160 in Fig. 3(b)), however, a two-layer microstructure is observed at both sides and the thickness of this layer increases

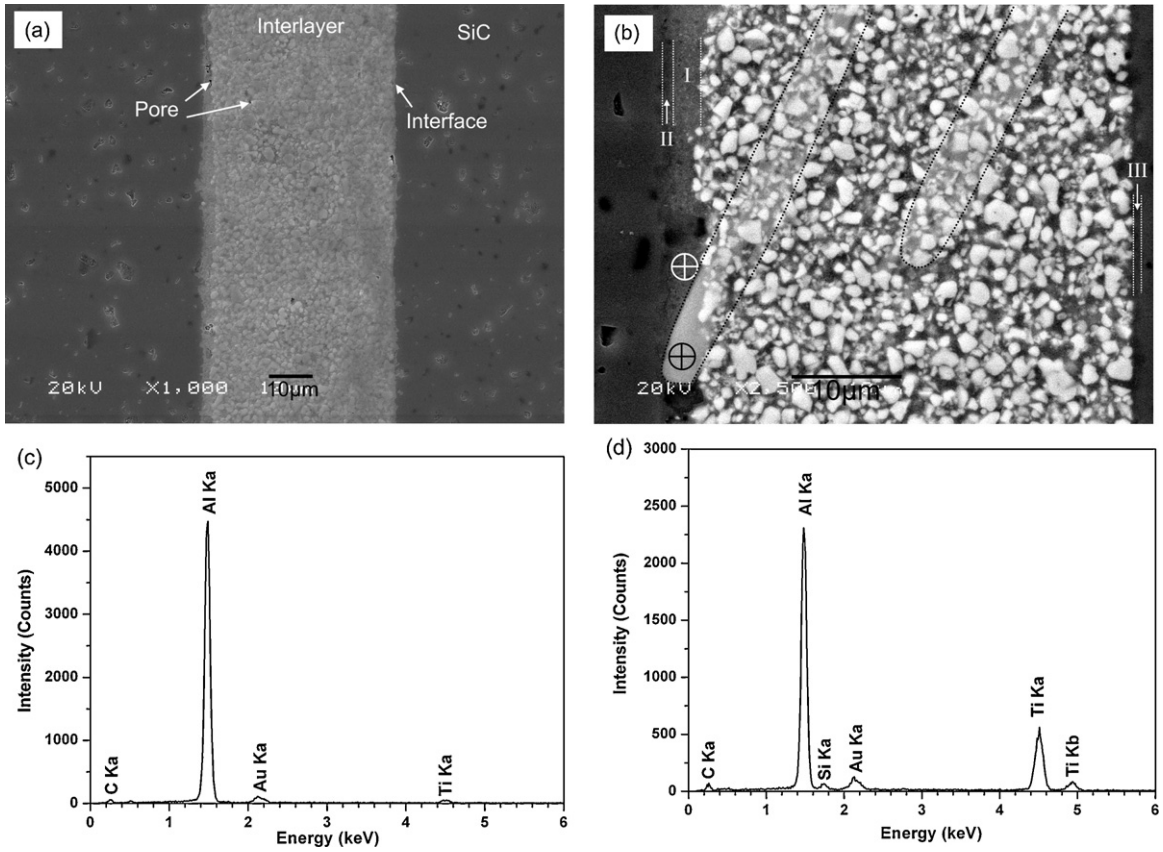


Fig. 2. (a) SEM and (b) backscattered SEM micrographs of the polished surface of SiC joint bonded at 1000 °C for 1 h by Al infiltrated TiC tape. EDS patterns of: (c) the white cross and (d) the black cross in (b).

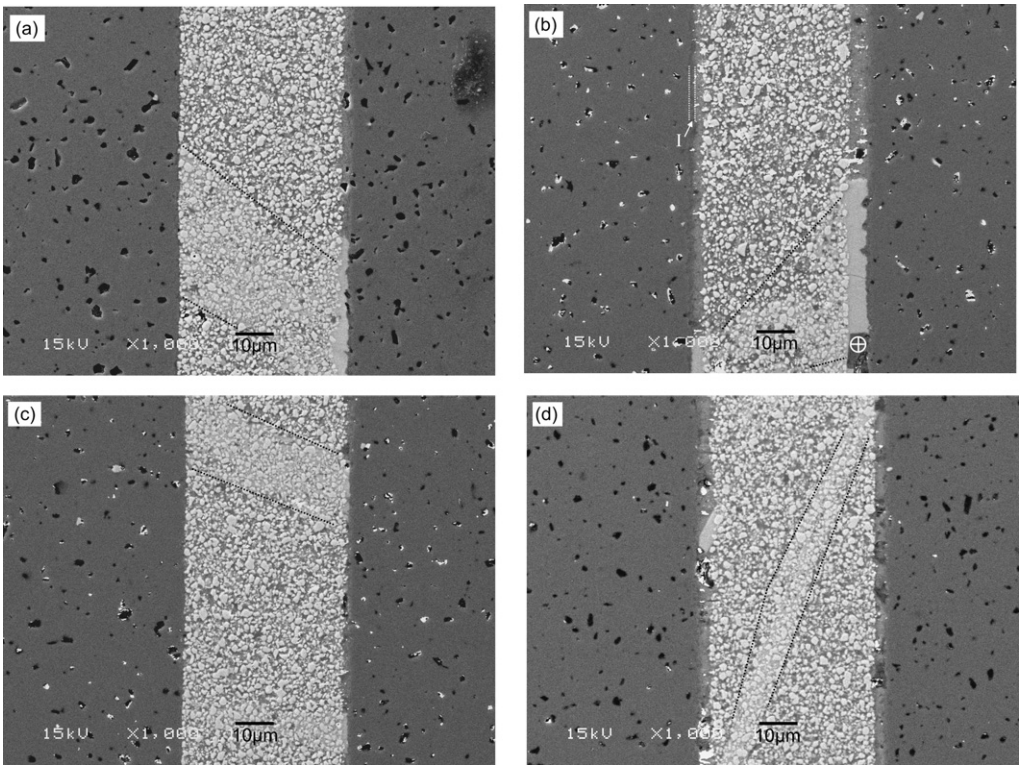


Fig. 3. Joining of SiC with Al infiltrated TiC tape at: (a) 900 °C for 1 h, (b) 1100 °C for 1 h, (c) 1000 °C for 0.5 h and (d) 1000 °C for 2 h.

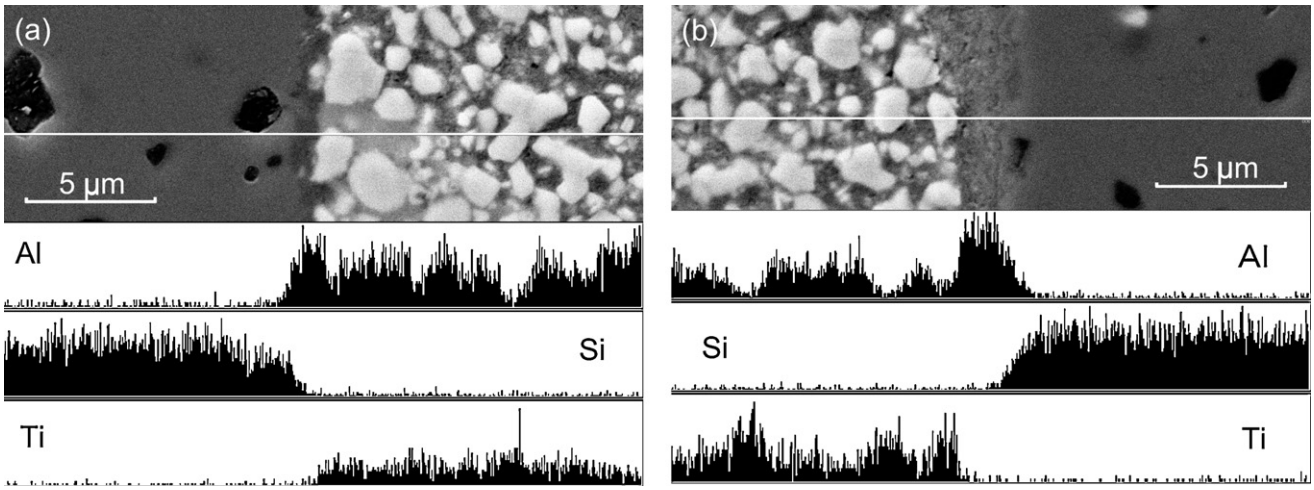


Fig. 4. EDS line-scan analysis on: (a) the one-layer interface and (b) the two-layer interfaces of SiC joint bonded at 900 °C for 1 h.

obviously. At the down side of right interface in Fig. 3(b), a dark gray grain marked by white cross connects the interlayer with SiC substrate. EDS analysis (not shown) suggests that the grain contains mostly Al, O and C elements, possibly the mixed compounds of $Al_2O_3$ and $Al_4C_3$. The $Al_2O_3$ might be a result of the reaction between Al and the absorbed oxygen in starting powder or the $SiO_2$ layer on the surface of SiC substrate. With extending the joining time to 2 h at 1000 °C (joint TCA102h in Fig. 3(d)), the microstructure similarly consists of a two-layer interface at both sides and contains some $Al_2O_3$–$Al_4C_3$ compound grains at interface. Also, the needle-like areas containing TiC and $TiAl_3$ are one of the evident microstructure features in all joints, as marked by black dot lines in Fig. 3(a) through (d).

To further clarify the difference between the one-layer and the two-layer interfaces, joint TCA960 was selected for the EDS line-scan analysis, with the results presented in Fig. 4(a and b). In the one-layer case (Fig. 4(a)), the reaction layer is generally composed of Al and Si elements and their content changes successively through this layer. Whereas in the two-layer side (Fig. 4(b)), besides the presence of a Al–Si layer close to SiC base, there exists another layer consisting of only Al with about 2 μm in thickness, which might be related to the low solubility of Si and Ti in the Al melt. These results indicate that the compositions of interfaces vary with their types and hence change their phase constituents, and finally affect their mechanical response.

Furthermore, based on the microstructure observations, we found that the joining temperature exhibits stronger influence on the growth rate of the interface layer thickness relative to the dwelling time, which is closely related to the mechanical performance of the prepared SiC joints. For example, joint TCA1160 exhibits the thickest interface layer and its reaction-formed layer shows a thickness of about 2 μm, as indicated by layer I in Fig. 3(b).

### 3.4. Mechanical properties and fracture surface observations of SiC joints

The dependence of bending strength on joining temperature is presented in Fig. 5(a), where the SiC joint strength keeps at about 240 MPa as joined at 900 °C and 1000 °C, and decreases to 190 MPa at 1100 °C. We also have prepared the joint at 1200 °C, but its strength is so low that the specimens fractured from interlayer during machining process. At a fixed temperature of 1000 °C, the effect of joining time on bending strength is depicted in Fig. 5(b). We found that the bending strength increases from 220 MPa to 240 MPa when extending the time from 0.5 h to 1 h, and keeps at this value up to 1.5 h. Further lengthening the time to 2 h leads to the increase of joint strength to 260 MPa. The quick decline of strength at high joining temperatures is attributed to the interface thickening and possibly the increased porosity in the interlayer for the evaporation of Al in vacuum.

From the opinion of fracture origin, joint TCA1160, namely the one having the lowest strength, generally fractures along the interlayer. In the other cases, SiC joints show a mixed fracture behavior, i.e. cracking from both the interlayer and SiC base. A typical fracture surface of joint TCA1060 is shown in Fig. 6(a), which consists of both gray area and bright area. Under higher magnification, as shown in Fig. 6(b), we found that the gray area shows the transgranular morphology of SiC base and the bright area exposes many intergranular faces. The fracture origin must be located in the bright area because the strength of joint TCA1060 (240 MPa) is lower than that of SiC substrate (450 MPa). EDS result suggests that the bright area contains Al–Si–O–C elements (Fig. 6(c)), indicating the presence of complicated reaction products, possibly including Si, $Al_4C_3$ and $Al_2O_3$. The reactions at Al/SiC interface have been reported in the literature and similar reaction products have been identified in details [28,29]. In fact, the bright area corresponds to the reaction-formed layer, e.g. layers II and III in Fig. 2(b) or layer I in Fig. 3(b).

The infiltration process and the joint microstructure are illustrated by a schematic in Fig. 7: Firstly, we setup a sandwich structure of SiC/TiC tape/SiC (Fig. 7(a)). As the temperature increases, the binder is burned away, leading to the shrinkage of interlayer. When Al melts, it infiltrates into the interlayer and fills the pores, as shown in Fig. 7(b). During infiltration, Al reacts

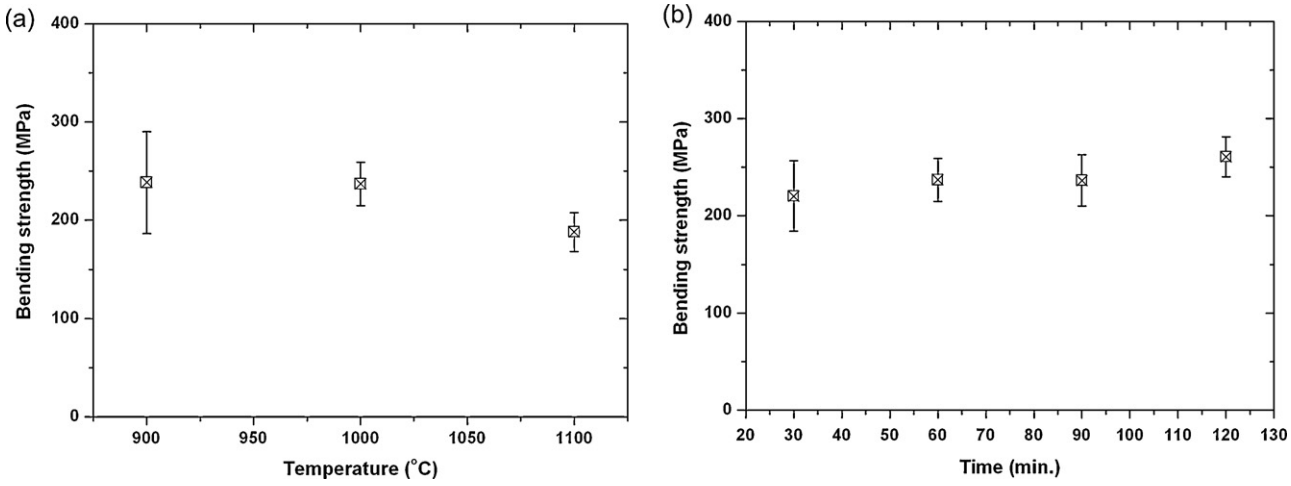


Fig. 5. The dependence of bending strength on: (a) different joining temperatures for 1 h and (b) varied joining time at 1000 °C.

with TiC and SiC simultaneously, forming $TiAl_3$ phase and a reaction-formed layer (Fig. 7(c)). $TiAl_3$ grains grow up to form a needle-like shape and the thickness of the reaction-formed layer increases with an increase in the joining temperature and time, as presented in Fig. 7(d).

Finally, it is worth to emphasize the most important aspects of the present study as follows: firstly, Al infiltrated TiC tape is found to be feasible for the joining of SiC and can produce SiC joint with strength higher than 190 MPa as bonded in the temperature range from 900 °C to 1100 °C for different time up to 2 h. Secondly, compared with the dwelling time, the joining temperature leads to the relatively quick growth of reaction-formed layer in thickness. Most importantly, the present results provide a candidate method for the production of large-sized

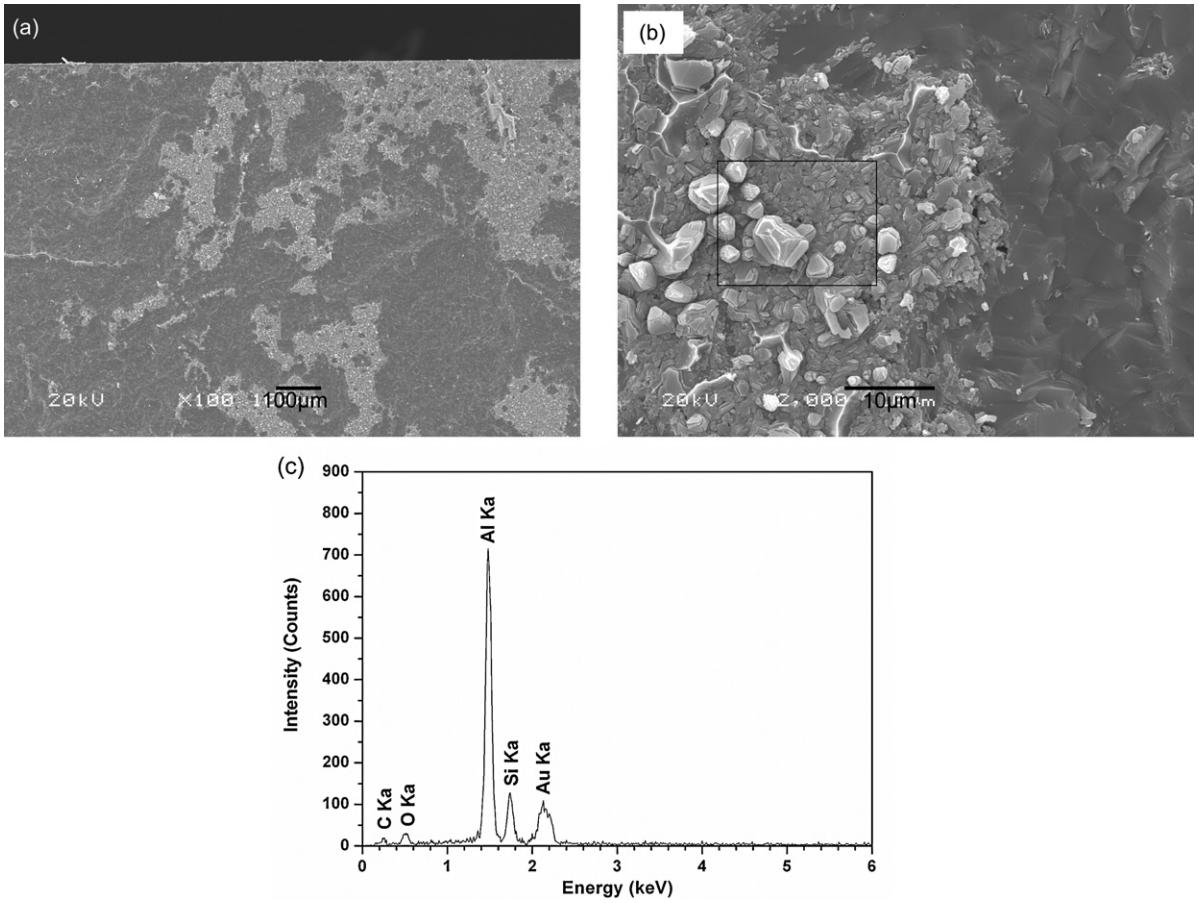


Fig. 6. (a) A typical fracture surface of SiC joint bonded at 1000 °C for 1 h by Al infiltrated TiC tape and (b) the fracture morphology at higher magnification. (c) EDS pattern of the area in (b) marked by a dark square.

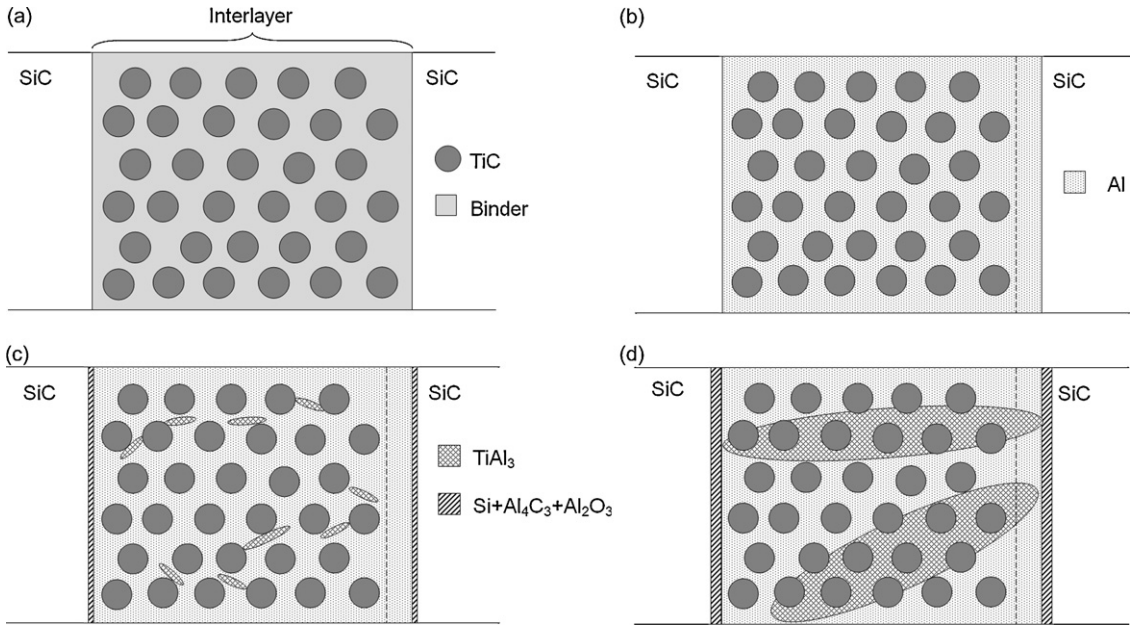


Fig. 7. A schematic on the microstructural evolution of interlayer during reactive infiltration process: (a) sandwich of SiC/TiC tape/SiC, (b) melt infiltration of Al into interlayer, (c) reactions between Al and TiC/SiC, (d) the growth of $TiAl_3$ grains and the thickening of reaction-formed layer.

engineering components and structures served at temperatures lower than 500 °C.

## 4. Conclusions

Commercially available SiC ceramics were successfully joined by Al infiltrated TiC tape at 900–1100 °C for 0.5 h to 2 h in vacuum. The SEM observations suggest that SiC joints show dense interlayer and crack-free interface. The phase constituents of the interlayer are predominantly composed of TiC and Al phases, together with a quantity of needle-like $TiAl_3$ alloy and trace amount of $Al_4C_3$ compound. The interface microstructure varies significantly with joining conditions. At low temperatures and short dwelling time, the interlayer contains a reaction-formed interface at one side and a two-layer structure, i.e. an Al-rich layer adding a reaction-formed layer, at the other side. With increasing the joining temperature and time, the two-layer microstructure is formed at both sides and its thickness increases significantly. The bending strengths of the prepared SiC joints are measured to be higher than 190 MPa. The significant decrease of strength with temperature is believed to be closely related to the interface microstructure and possibly the interlayer porosity.

## Acknowledgement

The present research was carried out with financial aid from New Energy and Industrial Technology Development Organization (NEDO) as part of the "Innovative Development of Ceramics Production Technology for Energy Saving". The authors would like to appreciate NEDO and all the other related parties for their support.

## References

1. Meetham GW. High-temperature materials: a general review. *J Mater Sci* 1991;**26**:853–60.
2. Munro RG. Material properties of a sintered alpha-SiC. *J Phys Chem Ref Data* 1997;**26**:1195–203.
3. Loehman RE, Tomsia AP. Joining of ceramics. *Am Ceram Soc Bull* 1988;**67**:375–80.
4. Fernie JA, Drew RAL, Knowles KM. Joining of engineering ceramics. *Int Mater Rev* 2009;**54**:283–331.
5. McDermid JR, Drew RAL. Thermodynamic brazing alloy design for joining silicon-carbide. *J Am Ceram Soc* 1991;**74**:1855–60.
6. Akselsen OM. Advances in brazing of ceramics. *J Mater Sci* 1992;**27**:1989–2000.
7. Asthana R, Singh M. Joining of $ZrB_2$-based ultra-high-temperature ceramic composites using Pd-based braze alloys. *Scripta Mater* 2009;**61**:257–60.
8. Rabin BH. Modified tape casting method for ceramic joining-application to joining of silicon-carbide. *J Am Ceram Soc* 1990;**73**:2757–9.
9. Rabin BH. Joining of silicon-carbide/silicon-carbide composites and dense silicon-carbide using combustion reactions in the titanium–carbon–nickel system. *J Am Ceram Soc* 1992;**75**:131–5.
10. Yajima S, Okamura K, Shishido T, Hasegawa Y, Matsuzawa T. Joining of SiC to SiC using polyborosiloxane. *Am Ceram Soc Bull* 1981;**60**, 253.
11. Zheng J, Ünal Ö, Akinc M. Green state joining of silicon carbide using polycarbosilane. *J Am Ceram Soc* 2000;**83**:1687–92.
12. Zheng J, Akinc M. Green state joining of SiC without applied pressure. *J Am Ceram Soc* 2001;**84**:2479–83.
13. DeLeeuw D. Effects of joining pressure and deformation on the strength and microstructure of diffusion-bonded silicon carbide. *J Am Ceram Soc* 1992;**75**:725–7.
14. Rabin BH, Moore G. Joining of SiC using reaction bonding methods. *Ceram Trans* 1992;**35**:291–9.
15. Hozer L, Lee JR, Chiang YM. Reaction-infiltrated, net-shape SiC composites. *Mater Sci Eng A* 1995;**195**:131–43.
16. Munoz A, Fernandez JM, Singh M. High temperature compressive mechanical behavior of joined biomorphic silicon carbide ceramics. *J Eur Ceram Soc* 2002;**22**:2727–33.
17. Iseki T, Kameda T, Maruyama T. Interfacial reactions between SiC and aluminum during joining. *J Mater Sci* 1984;**19**:1692–8.

18. Liu GW, Muolo ML, Valenza F, Passerone A. Survey on wetting of SiC by molten metals. *Ceram Int* 2010;**36**:1177–88.
19. Muscat D, Harris RL, Drew RAL. The effect of pore size on the infiltration kinetics of aluminum in titanium carbide preforms. *Acta Metall Mater* 1994;**42**:4155–63.
20. Tian WB, Kita H, Kondo N, Hyuga H, Nagaoka T. Effect of composition and joining parameters on microstructure and mechanical properties of silicon carbide joints. *J Ceram Soc Jpn* 2010;**118**:799–804.
21. Tian WB, Kita H, Hyuga H, Kondo N. Synthesis, microstructure and mechanical properties of reaction-infiltrated $TiB_2$–SiC–Si composites. *J Alloys Compd* 2011;**509**:1819–23.
22. Abramoff M, Magalhaes P, Ram S. Image processing with ImageJ. *Biophoton Int* 2004;**11**:36–43.
23. Nukami T, Flemings MC. In situ synthesis of TiC particulate-reinforced aluminum matrix composites. *Metall Mater Trans A* 1995;**26**:1877–84.
24. Kennedy AR, Weston DP, Jones MI. Reaction in Al–TiC metal matrix composites. *Mater Sci Eng A* 2001;**316**:32–8.
25. Lee KB, Sim HS, Kwon H. Reaction products of Al/TiC composites fabricated by the pressureless infiltration technique. *Metall Mater Trans A* 2005;**36A**:2517–27.
26. Albiter A, Leon CA, Drew RAL, Bedolla E. Microstructure and heat-treatment response of Al-2024/TiC composites. *Mater Sci Eng A* 2000;**289**:109–15.
27. Yang B, Wang F, Zhang JS. Microstructural characterization of in situ TiC/Al and TiC/Al–20Si–5Fe–3Cu–1Mg composites prepared by spray deposition. *Acta Mater* 2003;**51**:4977–89.
28. Peteves SD, Tambuyser P, Helbach P, Audier M, Laurent V, Chatain D. Microstructure and microchemistry of the Al/SiC interface. *J Mater Sci* 1990;**25**:3765–72.
29. Shorowordi KM, Laoui T, Haseeb ASMA, Celis JP, Froyen L. Microstructure and interface characteristics of $B_4C$, SiC and $Al_2O_3$ reinforced Al matrix composites: a comparative study. *J Mater Process Technol* 2003;**142**:738–43.